Wageningen Academic Publishers

Detection of fungal infection in pistachio kernel by long-wave near-infrared hyperspectral imaging technique

K. Kheiralipour[1,2,3*], H. Ahmadi[2], A. Rajabipour[2], S. Rafiee[2], M. Javan-Nikkhah[4], D.S. Jayas[3] and K. Siliveru[3]

[1]Mechanical Engineering of Biosystems Department, Ilam University, Ilam 69315-516, Iran; [2]Mechanical Engineering of Agricultural Machinery Department, University of Tehran, Karaj 31587-77871, Iran; [3]Department of Biosystems Engineering, University of Manitoba, Winnipeg, MB R3T 2N2, Canada; [4]Department of Plant Protection, University of Tehran, Karaj 31587-77871, Iran; k.kheiralipour@ilam.ac.ir

Received: 16 February 2014 / Accepted: 20 April 2015

RESEARCH ARTICLE

Abstract

Hyperspectral imaging is a non-destructive technique with great capability to detect food defects and diseases. In this research, infection of pistachio kernels by two different isolates of *Aspergillus flavus*, KK11 and R5, was determined using long-wave near-infrared hyperspectral imaging. Seven fungal growing stages on pistachio kernels, for both isolates, were investigated. The features from the hypercubes of healthy and infected pistachios were extracted, selected and then used for classification by linear discriminant analysis and quadratic discriminant analysis (QDA) methods which were performed by 10-fold cross validation technique in MATLAB 2010a. The QDA model gave the highest classification accuracy for all classes (healthy and infected kernels by different fungi and at different stages). For classification of infection by different fungi at the last fungal growing stage, QDA had the accuracy of 91.7%. As KK11 is an aflatoxin-producing and R5 is a non-aflatoxin-producing fungus isolate, the importance of the technique to detect aflatoxin contamination in pistachio is significant.

Keywords: classification, fungal infection, hyperspectral imaging, long-wave near-infrared, pistachio

1. Introduction

One of the main problems of pistachio nut is aflatoxin contamination, which has adverse effects on food and economic security (Saremi *et al.*, 2007). Aflatoxins B_1, B_2, G_1 and G_2 are carcinogenic (Diener *et al.*, 1987) and are formed by certain strains of *Aspergillus flavus* and *A. parasiticus* (Ehrlich *et al.*, 2003) under favourable conditions (Georgiadou *et al.*, 2012).

Several imaging techniques including visible imaging (Davies, 2009), X-ray imaging (Mathanker *et al.*, 2013), thermal imaging (Gade and Moeslund, 2014; Manickavasagan *et al.*, 2008) and hyperspectral imaging (Dale *et al.*, 2013) were used for agricultural and food subjects. The latest imaging technology used for fungal detection is hyperspectral imaging (HSI). In this method conventional imaging and spectroscopy are integrated to get area spectrum information from regions of interest. HSI has been used by several researchers as a non-destructive technique (Gowen *et al.*, 2007; Mahesh *et al.*, 2015) for many applications. In this method, many images corresponding to a desired wavelengths are collected as a three dimensional matrix, called hypercube (Mahesh *et al.*, 2015). For detecting fungal infection by hyperspectral imaging, Gomez-Sanchis *et al.* (2008) showed the capability of the technique in detection of rottenness in mandarin caused by *Penicillium digitatum* fungus. They used 20 wavelengths to classify the healthy and rotten fruits. Qin *et al.* (2009) discriminated the canker disease in citrus. They obtained the images in 450-930 nm wavelength region. In another research to detect citrus canker, Qin *et al.* (2012) developed a real-time system to capture images at 730 and 830 nm. Del Fiore *et al.* (2010) used hyperspectral imaging to detect toxigenic fungi on maize. They reported that the technique significantly can differentiate healthy from fungal infected maize kernels. Singh *et al.* (2012) classified the images of healthy and fungal-infected wheat

kernels obtained from short-wave near-infrared (SWNIR), 700-1,100 nm; long-wave NIR (LWNIR), 1000-1,600 nm; and visible region of the electromagnetic spectrum. They reported that the combination of SWNIR and digital colour image features gave the best results.

To the best of our knowledge, no research has been conducted to detect fungal infection in pistachio kernels. In this research, an aflatoxin-producing and a non-aflatoxin-producing isolate of *A. flavus* fungi were used to infect the pistachio kernels. Also, seven fungal growing stages for each fungus were investigated.

2. Materials and methods

Sample preparation

The pistachio kernels from Akbari variety produced in Rafsanjan region, Kerman, Iran, were selected randomly for the study. For sterilising, the kernels were put in a litre of hypochlorite sodium 0.05% for 1 min. The kernels were separated and dried at room temperature for 10 min. A portion of them was considered as healthy sample. Other kernels were infected by *A. flavus* fungi. Infection was done by two isolates of *A. flavus*: KK11 and R5, separately. The KK11 isolate cannot generate aflatoxin but R5 isolate produces it.

To infect the kernels, two suspensions with 10^7 spores/ml were produced. In the first, a suspension of distilled water and KK11 isolate was produced and used for infection of several sterilised kernels. After that, a new suspension was produced from distilled water and R5 isolate to infect the remaining sterilised kernels. The kernels were placed and turned in the respective suspension for 30 s. The infected kernels were taken out from the suspension and placed in Petri dishes. The dishes were placed in an incubator at 30 °C for a week. To investigate the ability of the hyperspectral imaging for detecting the fungi at different stages of infection, the kernels were taken to acquire near-infrared hyperspectral data after each day. So, there were 7 infection stages for each isolate: infection stage 1 (one day after putting infected kernels in incubator), infection stage 2, …, and finally infection stage 7. As shown in Table 1, totally, 15 classes of pistachio kernels were examined: (1) healthy pistachio; (2) infection stage one by KK11; (3) infection stage two by KK11; …; (8) infection stage seven by KK11; (9) infection stage one by R5; …; and (15) infection stage seven by R5.

Data acquisition

A LWNIR hyperspectral imaging system (Figure 1) was used to obtain hypercubes of healthy and fungal infected kernels at different fungal growing stages. This equipment is the same as used by Singh *et al.* (2012).

The system included a camera, thermoelectrically cooled InGaAs (model SU640-1.7RT-D; Sensors Unlimited Inc., Princeton, NJ, USA), detector with 640×480 pixels, a 25 mm F1.4 C-mount lens (Electrophysics Corp., Fairfield, NJ, USA) and two VariSpec liquid crystal tunable filters (LCTFs; model MIR06; Cambridge Research and Instrumentation Inc., Woburn, MA, USA) connected to the camera. The acquiring range of the system was 900-1,700 nm with minimum resolution of 0.01 nm limited by the internal electronics controlling the LCTFs. The illumination part included two halogen-tungsten lamps (300 W; Ushio

Table 1. Pistachio classes according to fungi contamination with *Aspergillus flavus* KK11 or R5.

Class no.	Class type	Specification	No. of samples
1	healthy	healthy pistachio	35
2	infection stage one by KK11	1 day after infecting by KK11	27
3	infection stage two by KK11	2 days after infecting by KK11	45
4	infection stage three by KK11	3 days after infecting by KK11	48
5	infection stage four by KK11	4 days after infecting by KK11	48
6	infection stage five by KK11	5 days after infecting by KK11	48
7	infection stage six by KK11	6 days after infecting by KK11	48
8	infection stage seven by KK11	7 days after infecting by KK11	48
9	infection stage one by R5	1 day after infecting by R5	48
10	infection stage two by R5	2 days after infecting by R5	46
11	infection stage three by R5	3 days after infecting by R5	48
12	infection stage four by R5	4 days after infecting by R5	48
13	infection stage five by R5	5 days after infecting by R5	48
14	infection stage six by R5	6 days after infecting by R5	48
15	infection stage seven by R5	7 days after infecting by R5	48
Total			681

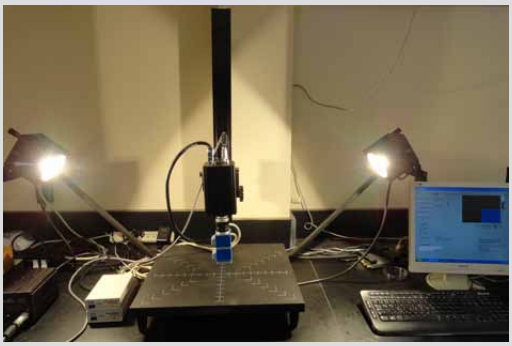

Figure 1. Long-wave near-infrared hyperspectral imaging system.

Lighting Inc., Cypress, CA, USA) placed at 0.5 m above the specimens with 45° downward angle. The camera was connected to a computer (Dell Optiplex GX280 Intel (R), Dell Inc., Round Rock, TX, USA) using a digital frame grabber (model NI PCI-1422; National Instruments Corp., Austin, TX, USA) through a RS-422 port. The system had a control program developed in LabVIEW environment (Version 1; National Instruments) for aligning the system, acquiring images and storing the obtained hyperspectral data (hypercube) in an addressable 12-bit binary file.

Before the commencement of each imaging session, a dark current image was acquired by putting the board in front of the lens to block the aperture of the camera. Thereby, the system could automatically subtract the dark current image from subsequent acquired images. To transform hypercubes into reflectance a standard Spectralon reflectance panel with 99% reflectance (Labsphere Inc, North Sutton, NH, USA) was used to acquire two white images at the start and the end of each imaging session (Singh *et al.*, 2012).

A black plastic board was used as a support to put samples in the front of the lens of the camera, and also to have a dark current image. Four non-contacted kernels were manually placed on the black plastic board under the lens of the camera. The control software was set to scan pistachio images at 960 nm to 1,700 nm with 10 nm intervals (totally 75 slices). To improve the signal to noise ratio, the system automatically acquired 10 image slices within each interval during image acquisition. For each pistachio class, the hypercubes of around 27-48 kernels were scanned. The acquired hypercubes were stored with corresponding names in an external hard drive attached to the personal computer.

Hyperspectral image processing

Image pre-processing and feature extraction

Three programs were developed in MATLAB (Mathworks Inc., Natick, MA, USA) to extract statistical features from the hypercubes. The first program calculated the average reflectance of the standard Spectralon reference from each imaging session. For this, the reflectance of all 75 wavelengths for both grabbed white images of each imaging session (at the start and the end of each session) were calculated and saved in a separate excel worksheet file with the corresponding name.

The second program obtained the first and second principal components, PC1 and PC2, of reflectance for each wavelength. These data were used to select the effective wavelengths for feature extraction according to Singh (2009).

The third program was for the extraction of statistical features only from the selected wavelengths. The features were maximum, mean, minimum, median, variance and standard deviation of reflectance of the hyperspectral images.

Image classification

The extracted features were considered as input to classifier algorithms which were developed based on linear discriminant analysis (LDA) and quadratic discriminant analysis (QDA) in MATLAB 2010a software. The discriminant analysis (DA) classifier discriminates the classes based on the predictor data. In DA, discriminant functions, estimated using training data, determine boundaries in predictor space between the classes. The generalised squared distance of average of each class is calculated and each response variable is assigned to a given class with a belonging probability. A multivariate normal density with an estimated pooled covariance is fitted to each class by LDA whereas QDA fits several multivariate normal densities with covariance estimates stratified by class (Chelladurai *et al.*, 2010; Singh *et al.* 2012).

K-fold cross validation technique was used to validate the developed LDA and QDA models. Cross validation or rotation estimation, divides the data to K groups and classification process is run K times. Each time, K-1 groups are used for training and the remaining group is used for validation (Bengio and Grandvalet, 2004). After K running times, all data were used for training and testing. As 10-fold was more popular (McLachlan *et al.*, 2004), in this research K was considered as 10.

3. Results and discussion

The first and second principal component factor loadings (PC1 and PC2, respectively) accounted for almost 99% total variance, and were separately plotted against the wavelengths for all classes. Figure 2 shows these data for PC1 (Figure 2A) and PC2 (Figure 2B), respectively. As PC coefficients or loadings explain the correlation between a component (e.g. PC1) and original variables (e.g. wavelength), the variable with highest absolute loading value in a particular component captures the maximum variance within that component. So, the top two wavelengths (1,090 and 1,280 nm) for PC1 factor loading (Figure 2A), and the highest factor loading wavelength (1,700 nm) for PC2 factor loading (Figure 2B) were selected as effective wavelengths for feature extraction (Kaliramesh *et al.*, 2013; Singh, 2009; Singh *et al.*, 2012).

The confusion matrix of the LDA and QDA classifiers are shown in Table 2 and 3, respectively. In each table, there were 15 different pistachio classes (Table 1). The correct classification rate (CCR) of the classifiers for classifying healthy and fungal infected pistachio kernels by KK11 and R5 isolates at various infection stages were 67.5 and 91.6% for LDA and QDA, respectively. The QDA model had higher ability to detect healthy pistachios and fungal infections isolates and stages than the LDA model.

As the CCR of QDA was higher than that of the LDA model, the confusion matrixes were different correspondingly. For example, classification accuracy to detect healthy pistachio from infected ones by QDA (35/35 or 100.0%) is significantly higher than that of LDA (32/35 or 91.43%). These results show the higher classification power of the QDA model to detect healthy from infected pistachio kernels. Also, classifying accuracy for detecting the class number 2 and 9 was 100%, whereas the classifier ability for other classes was lower.

Narvankar *et al.* (2009) reported that between statistical discriminant (linear, quadratic, and Mahalanobis) and back-propagation neural network methods for classification of soft X-ray images of healthy and infected wheat kernels by *Aspergillus niger*, *Aspergillus glaucus* group and *Penicillium spp.* in one growing stage, linear discriminant classifier was the best with accuracy of 98.9%. Delwiche (2003) used LDA, soft independent modelling of class analogy and the PCA to classify near-infrared reflectance spectroscopy data from sound and damaged wheat kernels. They reported that accuracy of LDA method was the highest (98.4%). This shows that the result of the present research (100.0% by HSI and QDA for healthy and infected pistachio) is comparable with the results of Delwiche (2003) and Narvankar *et al.* (2009).

Qin *et al.* (2009) discriminated canker disease in citrus using hyperspectral imaging technique with 96.2% accuracy. Gomez-Sanchis *et al.* (2008) classified healthy and fungal infected mandarin by hyperspectral imaging and reported that classification and regression trees method had the highest accuracy (around 91%). The best result reported by Peng *et al.* (2011) for prediction of microbial spoilage of beef using hyperspectral imaging was 95%. Wang *et al.* (2004) classified hyperspectral images of healthy and fungal infected soybean kernels. Their highest classification accuracy was 94.6%. Singh (2009) reached the highest accuracy for classification of hyperspectral images by combination of morphological, colour, textural and SWNIR features. His accuracy was between 99 and 100% for classification of healthy and fungal-infected wheat kernels.

By comparing the results of classification in the present study with the results of previous studies, although these

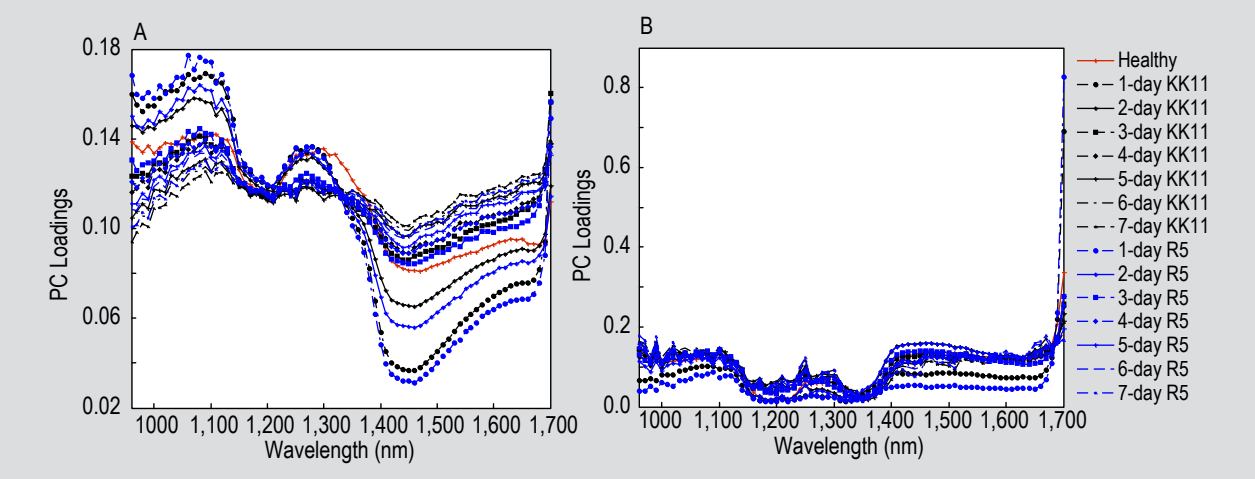

Figure 2. (A) First principal component (PC1) and (B) second principal component (PC2) data at different wavelengths for all classes, separately.

Table 2. Confusion matrix of the classifier model based on linear discriminate analysis.

Class no.[1]	1	2	3	4	5	6	7	8	9	10	11	12	13	14	15	Accuracy (%)
1	32	0	2	0	0	0	0	0	0	0	0	0	0	1	0	91.4
2	0	19	2	0	0	0	0	0	6	0	0	0	0	0	0	70.4
3	0	0	39	1	0	0	0	0	0	5	0	0	0	0	0	86.7
4	0	0	0	31	2	0	0	0	0	0	11	3	1	0	0	64.6
5	0	0	0	0	25	6	0	0	0	0	0	6	7	0	4	52.1
6	0	0	0	0	7	23	0	3	0	0	0	1	6	7	1	47.9
7	0	0	0	0	0	1	23	8	0	0	0	0	0	16	0	47.9
8	0	0	0	0	1	1	7	25	0	0	0	0	0	4	10	52.1
9	0	1	0	0	0	0	0	0	47	0	0	0	0	0	0	97.9
10	0	0	3	4	0	0	0	0	0	39	0	0	0	0	0	84.8
11	0	0	0	1	0	0	0	0	0	0	46	1	0	0	0	95.8
12	0	0	0	4	4	0	0	1	0	1	0	32	7	0	1	66.7
13	0	0	0	1	10	4	0	2	0	0	0	1	22	2	6	45.8
14	0	0	0	0	0	7	5	4	0	0	0	0	0	30	2	62.5
15	0	0	0	0	0	0	0	10	0	0	0	0	4	7	27	56.3
Accuracy (%)	100.0	95.0	84.8	73.8	51.0	56.1	65.7	47.2	88.7	86.7	80.7	72.7	53.7	44.8	52.9	67.5

[1] Description of classes is provided in Table 1.

Table 3. Confusion matrix of the classifier model based on quadratic discriminate analysis.

Class no.[1]	1	2	3	4	5	6	7	8	9	10	11	12	13	14	15	Accuracy (%)
1	35	0	0	0	0	0	0	0	0	0	0	0	0	0	0	100.0
2	0	27	0	0	0	0	0	0	0	0	0	0	0	0	0	100.0
3	0	0	43	0	0	0	0	0	0	2	0	0	0	0	0	95.6
4	0	0	0	43	0	0	0	0	0	0	3	2	0	0	0	89.6
5	0	0	0	1	38	0	1	1	0	0	0	5	1	1	0	79.2
6	0	0	0	0	1	42	2	0	0	0	0	0	0	1	2	89.6
7	0	0	0	0	0	2	44	0	0	0	0	0	0	2	0	87.5
8	0	0	0	0	0	0	6	34	0	0	0	0	1	0	7	70.8
9	0	0	0	0	0	0	0	0	48	0	0	0	0	0	0	100.0
10	0	0	0	0	0	0	0	0	0	46	0	0	0	0	0	100.0
11	0	0	0	1	0	0	0	0	0	0	47	0	0	0	0	97.9
12	0	0	0	0	3	0	0	0	0	0	0	45	0	0	0	93.8
13	0	0	0	1	0	0	0	1	0	0	0	0	43	0	3	89.6
14	0	0	0	0	1	0	1	0	0	0	0	0	0	46	0	95.8
15	0	0	0	0	1	0	0	2	0	0	0	0	2	0	43	89.6
Accuracy (%)	100.0	100.0	100.0	93.5	86.4	95.5	81.5	89.5	100.0	95.8	94.0	86.5	91.5	88.5	78.2	91.6

[1] Description of classes is provided in Table 1.

were not about pistachio, we conclude that hyperspectral imaging using QDA classifier can be a powerful machine vision technique for distinguishing healthy pistachio kernels from fungal infected ones (without considering fungus type and infection stage).

As can be seen in Table 2 and 3, the classification accuracy, adversely, decreased as time after infection increased. These results are counterintuitive but probably were caused by the non-homogeneity of fungal growth in the first days of infection. However, as the QDA had much better results than the LDA model, QDA method was followed for detecting 3 new classes without considering infection

time: (1) healthy pistachio; (2) pistachio infected by KK11 isolate at all stages; and (3) pistachio infected by R5 isolate at all stages (Table 4). The healthy pistachios and those infected by KK11 and by R5 were 35, 312 and 334 samples, respectively. As seen in Table 4, the QDA classifier can classify healthy kernels (35 of 35, 100.0%), infection by KK11 at all stages by accuracy of 285 of 312 (91.3%) and infection by R5 at all stages by 323 of 334 (96.7%). The CCR of the model for detecting the 3 classes was 94.4%. This result showed ability of hyperspectral imaging to detect the fungus effect, when comparing the healthy with infected kernels and also difference between fungus types, when comparing the infection by KK11 and R5 fungi isolates.

In order to investigate the possibility of hyperspectral imaging system with assistance of the QDA classifier for detecting aflatoxin contamination in pistachio, another classification was considered including 2 classes: (1) pistachio infected by KK11 isolate at stage seven (class number 8, including 48 specimens); and (2) pistachio infected by R5 isolate at stage seven (class number 15, including 48 specimens). The results are shown in Table 5. Here, the CCR of the classifier was 88.5%. The classifier can detect 40 of 48 infections by KK11 at stage seven and 45 of 48 infections by R5 at the same stage. The total error of the classifier was 11 of 96 (11.6%). As KK11 is an aflatoxin-producing and R5 is a non-aflatoxin-producing fungus, it seems that hyperspectral imaging techniques utilising this type of analysis procedure is a promising method to detect aflatoxin contamination in pistachio kernels.

Table 4. Result of quadratic discriminate analysis for classification of healthy pistachios and pistachios infected by *Aspergillus flavus* KK11 or R5 at all stages.[1]

	Class 1	Class 2	Class 3	Accuracy
Class 1	35	0	0	100.0%
Class 2	0	285	27	91.3%
Class 3	0	11	323	96.7%
Accuracy	100.0%	96.3%	92.3%	94.4%

[1] Class 1, 2 and 3 are healthy, *A. flavus* KK11 and R5, respectively.

Table 5. Result of quadratic discriminate analysis for classification of healthy pistachios and pistachios infected by *Aspergillus flavus* KK11 or R5 at the seventh stage.[1]

	Class 8	Class 15	Accuracy
Class 8	40	8	83.3%
Class 15	3	45	93.8%
Accuracy	93.0%	94.9%	88.54%

[1] Class 8 and 15 are healthy, *A. flavus* KK11 and R5, respectively.

4. Conclusions

Hyperspectral images of healthy and infected pistachio kernels by R5 and KK11 isolates of *A. flavus* fungi at seven fungal growing stages (totally 15 classes) were classified using LDA and QDA methods applied by 10-fold cross validation. Hyperspectral imaging by help of the QDA classifier successfully classified healthy and fungal infection of pistachio kernels without considering type of fungal isolate and infection stages (100% accuracy). Also, QDA method classified healthy and infected pistachios considering fungi type (KK11 and R5) by accuracy of 94.4%. The QDA procedure classified KK11 and R5 infection at last infection stage with accuracy of 88.5%. It seems that hyperspectral imaging technique utilising this type of analysis procedure is a promising method to detect aflatoxin contamination in pistachio kernels.

Acknowledgements

We thank the Natural Sciences and Engineering Research Council of Canada, Canada Foundation for Innovation, Manitoba Research and Innovation Fund, University of Manitoba, Winnipeg, Manitoba, Canada, Iran Ministry of Science, Research and Technology, Iran's National Foundation Elites and University of Tehran, Tehran, Iran, for partial support of this study. Special thanks to Dr. Malihipour and Messrs. Ahmad Alizadeh, Chelladurai Vellaichamy, C.B. Singh and Colin Demianyk for their technical assistance.

References

Bengio, Y. and Grandvalet, Y., 2004. No unbiased estimator of the variance of k-fold cross-validation. Journal of Machine Learning Research 5: 1089-1105.

Chelladurai, V., Jayas, D.S. and White, N.D.G., 2010. Thermal imaging for detecting fungal infection in stored wheat. Journal of Stored Products Research 46: 174-179.

Dale, L.M., Thewis, A., Boudry, C., Rotar, I., Dardenne, P., Baeten, V. and Fernández Pierna, J.A., 2013. Hyperspectral imaging applications in agriculture and agro-food product quality and safety control: a review. Applied Spectroscopy Reviews 48: 142-159.

Davies, E.R., 2009. The application of machine vision to food and agriculture: a review. The Imaging Science Journal 57: 197-217.

Del Fiore, A., Reverberi, M., Ricelli, A., Pinzari, F., Serranti, S., Fabbri, A.A., Bonifazi, G. and Fanelli, C., 2010. Early detection of toxigenic fungi on maize by hyperspectral imaging analysis. International Journal of Food Microbiology 144: 64-71.

Delwiche, S.R., 2003. Classification of scab and other mould damaged wheat kernels by near-infrared reflectance spectroscopy. Transactions of ASAE 46: 731-738.

Diener, U.L., Cole, R.J., Sanders, T.H., Payne G.A., Lee, L.S. and Klich, M.A., 1987. Epidemiology of aflatoxin formation by *Aspergillus flavus*. Annual Review of Phytopathology 25: 249-270.

Ehrlich, K.C., Montalbano, V.G. and Cotty, P.J., 2003. Sequence comparison of *aflR* from different *Aspergillus* species provides evidence for variability in regulation of aflatoxin production. Fungal Genetics and Biology 38: 63-74.

Gade, R. and Moeslund, T.B., 2014. Thermal cameras and applications: a survey. Machine Vision and Applications 25: 245-262.

Georgiadou, M., Dimou, A. and Yanniotis, S., 2012. Aflatoxin contamination in pistachio nuts: a farm to storage study. Food Control 26: 580-586.

Gomez-Sanchis, J., Gomez-Chova, L., Aleixos, N., Camps-Valls, G., Montesinos-Herrero, C., Molto, E. and Blasco, J., 2008. Hyperspectral system for early detection of rottenness caused by *Penicillium digitatum* in mandarins. Journal of Food Engineering 89: 80-86.

Gowen, A.A., O'Donnell, C.P., Cullen, P.J., Downey, G. and Frias, J.M., 2007. Hyperspectral imaging-an emerging process analytical tool for food quality and safety control. Trends in Food Science and Technology 18: 590-598.

Kaliramesh, S., Chelladurai, V., Jayas, D.S., Alagusundaram, K., White, N.D.G. and Fields, P.G., 2013. Detection of infestation by *Callosobruchus maculatus* in mung bean using near-infrared hyperspectral imaging. Journal of Stored Products Research 52: 107-111.

Mahesh, S., Jayas, D.S., Paliwal, J. and White, N.D.G., 2015. Hyperspectral imaging to classify and monitor quality of agricultural materials. Journal of Stored Products Research 61: 17-26.

Manickavasagan, A., Jayas, D.S., White, N.D.G. and Paliwal, J., 2008. Wheat class identification using thermal imaging: a potential innovative technique. Transactions of the ASABE 51: 649-651.

Mathanker, S.K., Weckler, P.R. and Bowser T.J., 2013. X-ray applications in food and agriculture: a review. Transactions of the ASABE 56: 1227-1239.

McLachlan, G.J., Do, K.A. and Ambroise, C., 2004. Analyzing microarray gene expression data. 2004. Wiley, New York, NY, USA.

Narvankar, D.S., Singh, C.B., Jayas, D.S. and White, N.D.G., 2009. Assessment of soft X-ray imaging for detection of fungal infection in wheat. Biosystems Engineering 103: 49-56.

Peng, Y., Zhang, J., Wang, W., Li, Y., Wu, J., Huang, H., Gao, X. and Jiang, W., 2011. Potential prediction of the microbial spoilage of beef using spatially resolved hyperspectral scattering profiles. Journal of Food Engineering 102: 163-169.

Qin, J., Burks, T.F., Ritenour, M.A. and Bonn, G.W., 2009. Detection of citrus canker using hyperspectral reflectance imaging with spectral information divergence. Journal of Food Engineering 93: 183-191.

Qin, J., Burks, T.F., Zhao, X., Niphadkar, N. and Ritenour, M.A., 2012. Development of a two-band spectral imaging system for real-time citrus canker detection. Journal of Food Engineering 108: 87-93.

Saremi, H., Okhovvat, M. and Saremi, H., 2007. Control managements of *Aspergillus flavus* a main aflatoxin producers and soil borne fungi on pistachio in Kerman. Iranian Food Science and Technology Research Journal 3: 27-31.

Singh, C.B., 2009. Detection of insect and fungal damage and incidence of sprouting in stored wheat using near-infrared hyperspectral and digital color imaging. Ph.D. dissertation. University of Manitoba, Winnipeg, Canada.

Singh, C.B., Jayas, D.S., Paliwal, J. and White, N.D.G., 2012. Fungal damage detection in wheat using short-wave near-infrared hyperspectral and digital colour imaging. International Journal of Food Properties 15: 11-24.

Wang, D., Dowell, F.E., Ram, M.S. and Schapaugh, W.T., 2004. Classification of fungal-damaged soybean seeds using near-infrared spectroscopy. International Journal of Food Properties 7: 75-82.